Duplex Stainless Steel Self-ligating Orthodontic Brackets by Micro-powder Injection Moulding

María E. Sotomayor[1], Alberto Cervera[2], Alejandro Várez[3*], Belén Levenfeld[4]

[1,3,4]Departamento de Ciencia e Ingeniería de Materiales, Universidad Carlos III de Madrid, Madrid, SPAIN
[2]Euroortodoncia SA, Madrid, SPAIN

Abstract— *This work deals with the production of duplex stainless steel dental brackets by micro-powder injection moulding employing a thermoplastic binder based on high density polyethylene and paraffin wax. The starting powder was a mixture of ferritic and austenitic gas-atomized powders in a volume ratio of 50/50. Feedstocks with powder loadings of 50, 60, 65 and 68 vol.% were prepared. All feedstock compositions presented a pseudoplastic flow behaviour. The critical powder volume concentration experimentally determined through oil absorption method and applying a rheological model was 71 vol.%. A mixture with a 65 vol.% of solid loading was chosen to perform the complete route. Injection moulding stage was successfully carried out and green parts were obtained with an accurate dimensional precision. Green brackets were thermally debound under a cycle developed on the basis of thermogravimetric analysis. The cycle took place under argon atmosphere to prevent the oxidation of metallic powder and it lasted only 4 hours. Samples were successfully sintered in low vacuum at 1250ºC, final parts reached densities close to 98%. Scanning electron micrographs revealed a biphasic microstructure distinctive of duplex stainless steels.*

Keywords— duplex stainless steel, thermoplastic binder, micro-powder injection moulding.

I. INTRODUCTION

A few years ago micro-powder injection moulding (µ-PIM) became a manufacturing process of growing interest gaining importance in several fields as automotive, electronics and medical technology. This process is one of the key technologies for manufacturing 3D near net shape micro-components. Adapted from PIM, µ-PIM allows processing of stainless steel powders through a profitable and advantageous method for the fabrication of micro-components with a high shape complexity [1]. This process consists of similar steps than PIM: mixing, injection moulding, debinding and sintering [2]. It begins with a suitable selection of powder and binder components. In the case of µ-PIM, the starting powder must be small enough to replicate the finest details, and multicomponent binder systems are normally used to meet the requirements for the process success. Usually, multicomponent binders constituted of polymers and other additives improve the debinding process: the binder removal occurs in a wider temperature range and in a more gradual way. The powder and binder are mixed together to obtain a mixture called feedstock. The feedstock should have low viscosity for filling the micro-cavities and enough strength for avoiding the breaking of the pieces during ejection process. After moulding, the binder is removed to obtain the so-called "brown part" that retains the original shape, and finally it is sintered to shrink in an isotropic way till near full density.

A specific application of µ-PIM in medical technology is dental brackets [3]. Orthodontic brackets are precision parts where the arch slot tolerances must be maintained. On the other hand, each tooth demands its own bracket. In this sense, PIM is a powerful tool to obtain this kind of pieces through an advantageous method as it was demonstrated for alumina brackets [4]. The choice of materials available in orthodontics depends on factors such as physical, mechanical and biological properties. Plastic brackets are esthetically satisfying but have several undesirable effects such as high wear and failure to deliver sufficient torque because of their low modulus. Aesthetic ceramic brackets provide significantly better mechanical properties, increased transparency [5], and decreased reactivity with the oral environment than plastic brackets. Finally, stainless steel has been proved to be a very good material for orthodontic appliances due to its low cost, greater strength, higher modulus of elasticity, good formability, and high corrosion resistance in the mouth. The austenitic stainless steel alloy 316L, which is used primarily for bracket manufacturing, contains nickel in the range of 10-14 wt.%. Metal brackets have in general good strength but possess some problems associated with the allergenic potential of nickel, whose allergic effects are well described nowadays. On the other hand, pitting corrosion of orthodontic appliances is common due to the aggressive action of Cl^- ions in saliva, or from food and drink [6]. Furthermore, when the bracket and wire are combined with a ligature wire, crevice and galvanic corrosion can occur, and further types of corrosion may develop when the bracket is soldered to the metal band. The release of Ni ions, as a consequence of corrosion process, could cause adverse effects. Their predominant

systemic effects in humans are allergies, dermatitis, and asthma [7]. Recently it has become apparent that there is a need for higher corrosion resistance, greater mechanical strength, improved formability and lower cytotoxicity.

However, because nickel has an essential role in the stabilization of the austenitic phase and in the corrosion resistance of stainless steels, it is difficult to remove nickel totally. Several alloys as super stainless steels have been proposed for orthodontic applications. In vitro nickel-ion release testing was carried out in artificial saliva in super stainless steels and it was determined that the nickel-ion release property depends on the properties of the passive film [7].

In this sense, duplex stainless steels (DSS) have been proposed in this work as materials with very high mechanical properties and lower nickel content. Moreover, the corrosion characteristics of DSS (i.e. 2205) were demonstrated to be better than those of austenitic stainless steel (i.e. 316L) in artificial saliva [8]. Even their toughness is higher than that of the ferritic steels but slightly lower than the austenitic ones [9]. DSS are characterized by a structure consisting of approximately equal amounts of ferrite and austenite. This kind of steels can be obtained by powder metallurgy premixing ferritic and austenitic powders in the adequate proportion [10-17].

The brackets, here analyzed, belong to self-ligating brackets and they are constituted of a base body and a tap. Combined with the introduction of PIM manufacture, which permits closer tolerances, the development of new designs is possible. Some of the proposed advantages of employment self-ligating brackets are summarized in these points [18, 19]:

- More certain full archwire engagement.
- Low friction between the bracket and the archwire.
- Less chairside assistance needed.
- Faster archwire removal and ligation.

The aim of this work is producing near net-shape duplex stainless steel brackets by µ-PIM. For this purpose, a feedstock with a thermoplastic binder based on high density polyethylene and paraffin wax was employed. The optimization of the different stages of the manufacturing process is described besides the characterization of final parts.

II. EXPERIMENTAL SECTION

2.1 Materials

A premixed 316L and 430L gas-atomized powder in a volume ratio of 50/50 was employed in this work. A scanning electron micrograph of powder is presented in Fig. 1 where the near spherical morphology can be observed. Particle size and particle size distribution of powder affect the different stages of the PIM process [20]. So, particle size distribution obtained in a Malvern Mastersizer 2000 laser scattering particle analyzer is shown (d_{90} = 9.1µm, d_{50} = 5.5 µm, d_{10} = 3.2 µm). The pycnometric density of powder was 7.82 g/cm^3.

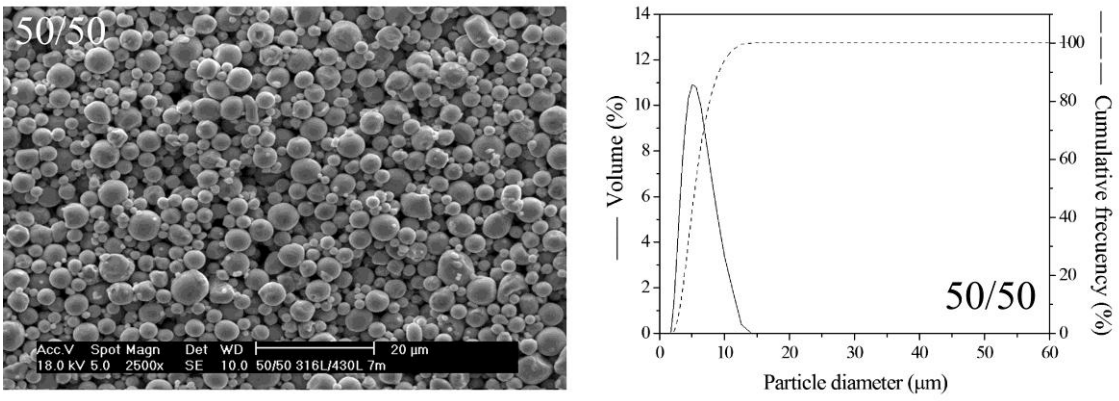

FIGURE 1. SCANNING ELECTRON MICROGRAPH AND PARTICLE SIZE DISTRIBUTION OF STARTING POWDER.

A thermoplastic binder system previously developed was employed in this work [21]. It was composed of high density polyethylene (HDPE) and paraffin wax (PW) in a volume ratio of 50/50. HDPE retains the shape of injected parts and PW decreases viscosity and improves flowability of melted mixture. The melting temperatures of HDPE and PW were 131 and

53 ºC, and decomposition temperature ranges of both components were 100 and 95 ºC (see Reference 21 for further details of binder).

2.2 Feedstock preparation

A Haake Rheocord 252p mixer equipped with a pair of rotating blades was employed for the preparation of feedstocks. Mixing temperature, rotation speed, and mixing time were adjusted at 170 ºC, 40 r.p.m. and 45 min, respectively. The maximum capacity of the mixing chamber was 69 cm^3 and a 70% of this volume was filled. Mixing torque evolution against time was recorded to evaluate the mixing process. Four mixtures were prepared with powder loadings of 50, 60, 65 and 68 vol.%.

In order to produce larger batches for the injection moulding stage, compounding of powder and binder was carried out in a Haake Rheomex CTW100p twin-screw extruder. The temperature profile along the barrel was 160/165/170 ºC, and the rotation of the screws was set at 70 r.p.m. A highly homogeneous feedstock was obtained after three extrusion steps.

2.3 Feedstock rheology and CPVC measurement

A Haake Rheocap S20 capillary rheometer was employed to determine the rheological behaviour of feedstocks. A 1 mm diameter and 30 mm length die was used. Shear rates were varied from 100 to 10000 s^{-1}, and 10 minutes were allowed to reach thermal equilibrium after charging the barrel.

The determination of critical powder volume concentration (CPVC) is important in order to establish the optimum amount of binder in the feedstock. The CPVC was determined by means of two methods: through rheological measurements applying Reddy theoretical model [22], and by oil absorption experimental method developed by Bierwagen [23] and Mutsuddy and Ford [24] using torque measurement during mixing.

Several mathematical models have been proposed to predict the maximum volume fraction of the filler from rheological measurements. In the case of PIM, the Reddy model was previously applied to evaluate the CPVC [17, 20]. The model equation is given as follows:

$$\eta\phi_b = \eta(\phi_b)_m + \eta_b(1-(\phi_b)_m) \tag{1}$$

where η is the mixture viscosity; η_r is the relative viscosity; η_b is the binder viscosity; $\eta_r = \eta / \eta_b$; ϕ is the filler volume fraction; ϕ_m is the maximum filler loading; ϕ_b is the binder volume fraction; and $(\phi_b)_m$ is the critical binder volume fraction.

On the other hand, the oil absorption method gave successful results in another system that previously we developed. It was successfully employed to determine CPVC in a feedstock based on ferritic and austenitic powders with a particle size close to 22 μm [17]. It consists in loading the mixer chamber with a premeasured volume of dry powder at room temperature with a constant rotation speed of rotor blades. Subsequently, the oil was added stepwise to the camera and the torque is recorded continuously as a function of time. With the addition of liquid, torque increases gradually until a maximum is reached. If the addition of oil continues the torque value decreases abruptly indicating that the critical powder volume concentration is reached. CPVC is defined by (2) using powder volume V_p and liquid phase volume V_L, at the point where torque is a maximum:

$$CPVC = \frac{V_p}{V_p + V_L} \tag{2}$$

The rotation speed was maintained at 50 r.p.m. and an aliquot of 2 ml of oil was added at regular intervals into the chamber.

2.4 Injection moulding

A Battenfeld Microsystem 50 injection moulding machine was employed in this stage. Every part of the bracket was injected in a different mould and the geometry of the cavities can be shown in Fig. 2. Suitable processing parameters including temperature, volume and injection speed were optimized to ensure a complete filling.

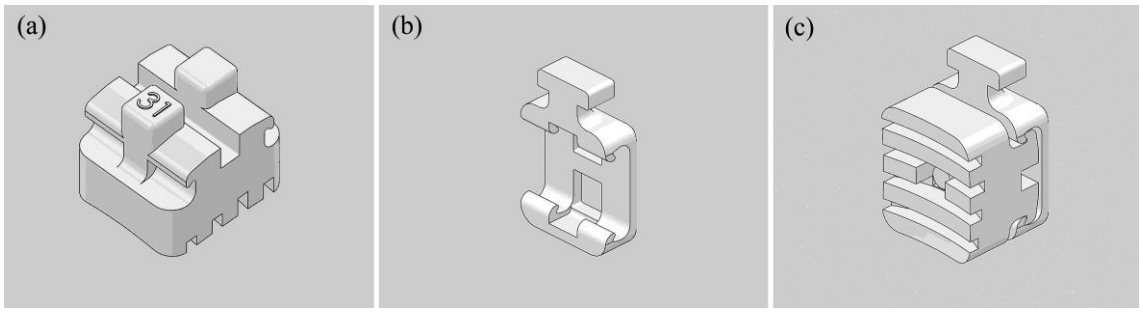

FIGURE 2. GEOMETRY OF THE SELF-LIGATING BRACKET: (A) THE BASE, (B) THE TAP AND (C) BOTH PARTS TOGETHER.

2.5 Debinding and sintering

Binder removal was carried out under a thermal cycle in a Goceram GC-DC-50 furnace. This cycle was designed on the basis of the previous thermogravimetric analysis (TGA) of the feedstock. TGA was performed using a Perkin Elmer Pyris 1 instrument, and decomposition temperature range of polymer and additives was determined. In order to assure the complete removal of binder the carbon content of debound samples was determined using a LECO CS-200 instrument. Parts were sintered in low vacuum ($<10^{-2}$ mbar) at 1250 ºC for 1h employing a heating rate of 5 ºC/min. Sintered parts were electrochemical etched with KOH 3M to observe the microstructure.

III. RESULTS AND DISCUSSION

3.1 Mixing

Fig. 3 illustrates the mixing behavior of the feedstocks with volumetric powder loading of 50, 60, 65 and 68%. The mixing torque, proportional to the shear stress of the mixer, indicates the work energy consumed to disperse and distribute the powder in the binder [25].

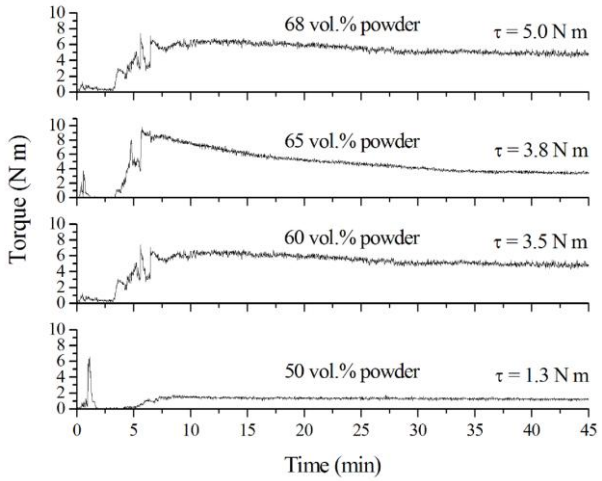

FIGURE 3. EVOLUTION OF TORQUE AGAINST MIXING TIME FOR FEEDSTOCKS WITH DIFFERENT POWDER LOADINGS.

At the initial stage, additions of binder components were realized. Afterwards, powder was added and higher fluctuations were produced in torque value. Once all the powder was added, the feedstocks achieved the steady state in a mixing time below 30 minutes. This steady state torque (τ) is reached when mixture is homogeneous. Steady state torque has been calculated taking into account the last 5 minutes of the process and the mean value has been reported. This parameter increases from 1.3 to 5.0 N·m when powder loading increases as a consequence of the higher viscosity of the mixture.

Heterogeneous mixtures produce density gradients. So, in order to quantify the homogeneity degree of feedstocks to obtain high-quality final pieces, a previous study of density was carried out. The pycnometric density of different portions of feedstock from the same batch was measured. Fig. 4 shows pycnometric density for each feedstock determined as the mean

value of 5 samples. The standard deviation of each value was also plotted (as error bars). As expected, density of feedstock increased with powder loading, and it could be concluded that homogeneity was high because the standard deviation was lower than 0.1%. On the other hand, a good agreement between experimental and calculated values on the basis of rule of mixing is found. So, there was no loss of any component during mixing process.

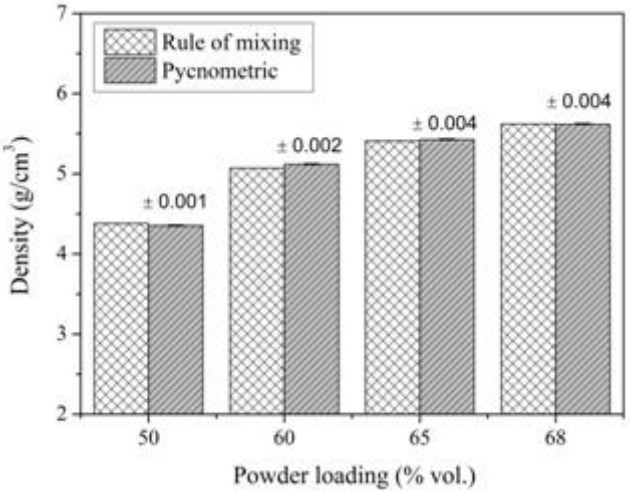

FIGURE 4. PYCNOMETRIC AND THEORETICAL DENSITIES OF FEEDSTOCKS.

Torque variation during the CPVC test as a function of mixing time is plotted in Fig. 5(a). Initially, when an aliquot of oil is added to powder, the torque rises sharply due to the immediate mobilization of the liquid by the powder particles to form a few big clusters. Considerable stresses are therefore required in order to break these clusters. Thus, during mixing at a constant shear rate, high torque values are encountered initially when only a few big clusters are present. As the addition of liquid continues, the mean equilibrium size of the clusters becomes bigger and bigger as more and more particles join together, until ultimately the whole mass becomes a coherent paste. Corresponding to this, the torque also continuously increases until it reaches a peak at the point of CPVC. From then on, further addition of any liquid serves only to dilate the solid structure and increase the interparticle distances. Therefore, the mixing torque falls as shown in Fig. 5(a).

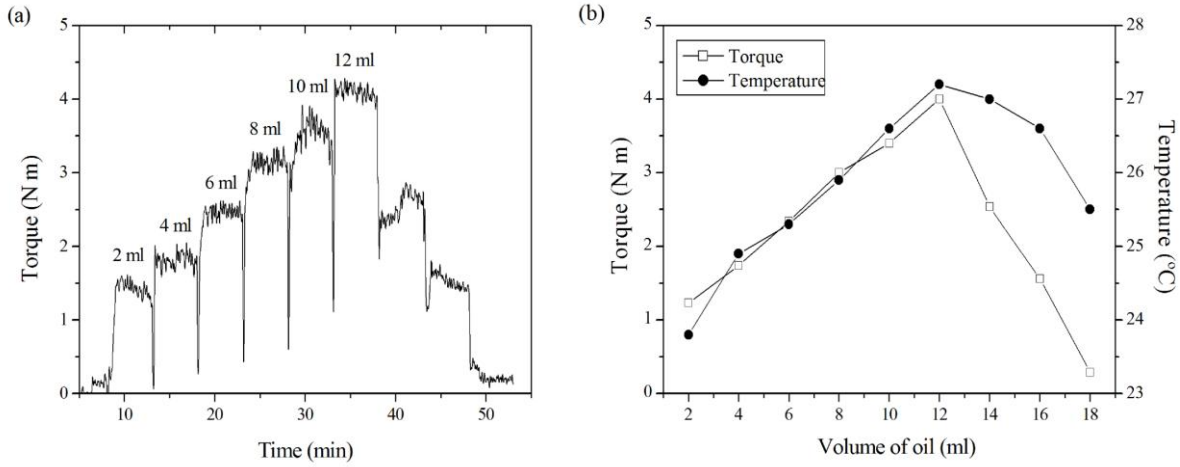

FIGURE 5. (A) TORQUE VARIATION WITH MIXING TIME FOR DIFFERENT ADDITIONS OF OIL; (B) TORQUE AND TEMPERATURE VALUES FOR DIFFERENT OIL VOLUMES.

In Fig. 5(b) torque and temperature values corresponding to increasing additions of oil are represented. In our case, the maximum is reached with the addition of 12 ml of oil. The temperature will not rise on subsequent oil addition, as there is no further decrease in surface energy, and the capillary forces, also begin to decrease as the excess liquid can only separate the particles. With any further oil addition the temperature falls as the surface forces become ineffective. According to this experimental method, the CPVC for this system is 72 vol.%. A CPVC of 72 vol.% was obtained in previous experiments

realized with a similar powder with a d_{90} of 21 μm [17], so it can be concluded that this method is not enough sensitive to differentiate this change of particle size.

Besides the previous studies of torque realized, a study of viscosity was performed in order to choose the most suitable feedstock to be injected. The variation of viscosity values with the shear rate is presented in Fig. 6. As it was expected, when powder loading increases viscosity increases too. In all the samples viscosity decreases with shear rate according to a pseudoplastic behavior which is the most desirable for PIM process. This result states that powder particle size and its distribution strongly affect the viscosity of feedstock when comparing these values with the ones obtained in Reference 17.

The relationship between shear stress and shear rate in a pseudoplastic fluid can be described by the power law model proposed by Ostwald [26] and De Waele [27]. The power law model can be written as follows:

$$\tau = k\dot{\gamma}^n \tag{3}$$

where k is referred as the consistency index and n the power law index. In the case of a pseudoplastic behaviour, n<1. The value of n indicates the degree of sensitivity of viscosity against shear rate.

Pseudoplastic flow is often sought in the moulding process to ease mould filling, to minimize jetting, and for helping the shape retention of component [2]. However, some moulding defects such as jetting are also associated with high pseudoplastic character or low value of the exponent n of the power law. A high power law index indicates low shear sensibility and a low index indicates higher shear sensibility. The power law indexes obtained were 0.65, 0.51, 0.50 and 0.47 for feedstocks with powder loadings of 50, 60, 65 and 68 vol.% respectively. These values are high enough to assure that the mentioned defects will be avoided.

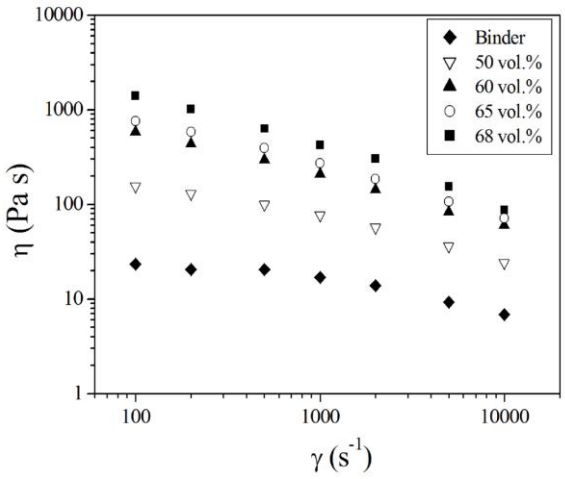

FIGURE 6. VISCOSITY CURVES OF BINDER AND FEEDSTOCKS WITH DIFFERENT POWDER LOADINGS AT 170°C.

An important fact is that the feedstocks with powder loadings of 50, 60 and 65 vol.% have viscosities under 1000 Pa·s in the shear rate range between 100 and 1000 s^{-1}, and it is widely known, that the most suitable behavior for injection moulding is given by mixtures that meet this requirement [28].

There is a good agreement of experimental data to the Reddy model. The fitting was realized with the viscosity data obtained at 100 s^{-1} and 170 ºC. The fit linear coefficient was 0.996 and CPVC was calculated from the slope. A value of 71 vol.% was obtained, similar than previously obtained employing the experimental oil absorption method. When we employed Reddy model to determine CPVC in a similar system with a powder with a d_{90} of 21 μm [17], a value of 72 vol.% was obtained. So, we can assure that sensitivity of this method to particle size is higher than oil absorption method.

Usually, the optimal solid loading contains more binder than the critical one and, this optimal loading is approximately 5-7% lower than critical [29]. In this way, the optimal loading should be close to 67-66 vol.%.

Finally, the mixture with the highest powder loading that exhibits a suitable viscosity is the feedstock with a 65 vol.%. As a consequence, and taking into account torque results and CPVC estimations, an optimum powder loading of 65 vol.% was selected to go on with the injection stage.

3.2 Injection moulding

Once the most suitable powder loading was chosen, a high amount of feedstock was obtained using the twin-screw extruder. Injection stage was carried out by controlling the main parameters such as barrel and mould temperatures, injection volume and injection speed. Firstly, the barrel temperature profile was adjusted at 160/165/170 ºC. This increasing temperature profile was chosen because it provides a decreasing viscosity profile to improve the delivery of feedstock to the die. The injection temperature is higher than melting temperature of HDPE but lower than degradation temperature of wax. On the other hand, mould temperature also played an important role in the complete filling of the cavity. When a low mould temperature was used an incomplete mould filling was observed. Best results were obtained at 45 ºC in the case of bracket-tap. However, in the case of the bracket-base a higher mould temperature (50 ºC) was needed in order to fill completely the cavity. Subsequently, the injection volume was varied in order to achieve a complete mould filling. The optimum injection speeds for bracket-tap and base were 100 and 120 mm/s, respectively. In this way, the bracket-body as much as the tap were successfully moulded and the optimized injection parameters are shown in Table 3.

TABLE 3
OPTIMIZED INJECTION MOULDING PARAMETERS OF BRACKET-TAP AND BASE.

	Tap	Base
Barrel temperature (ºC)	160/165/170	160/165/170
Mould temperature (ºC)	45	50
Injection speed (mm/s)	100	120
Injection volume (mm^3)	220	260

Micrographs of green bodies are shown in Fig. 7. In spite of the so complicated geometry, the shape of both parts was accurately reproduced. The edges of the micro-parts were well defined and in the case of the bracket-tap the central arm was fully filled. Fig. 7(b) shows an accurate definition of retention zone and wire slot of the bracket-base.

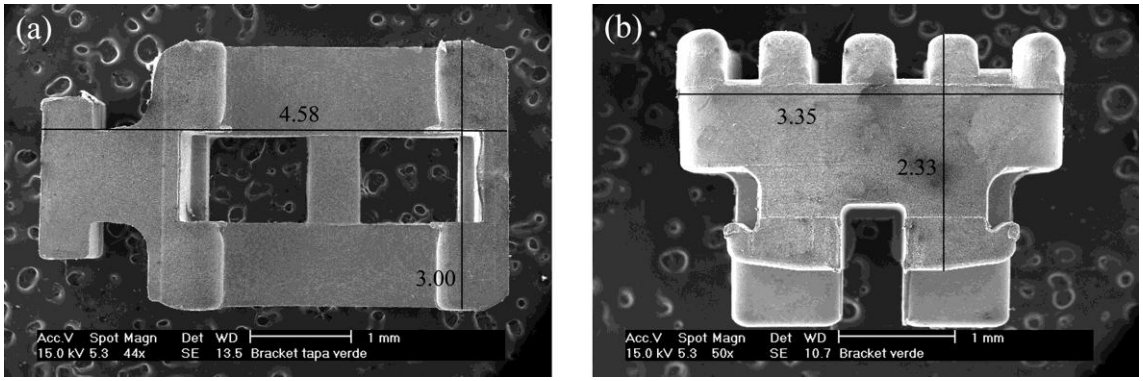

FIGURE 7. SCANNING ELECTRON MICROGRAPHS OF GREEN (A) TAP AND (B) BASE. DIMENSIONS ARE GIVEN IN MM.

3.3 Debinding

After injection process the optimization of debinding stage was carried out. A thermal debinding cycle was designed on the basis of thermogravimetric analysis of feedstock (see Fig. 8(a)). The first dwell step at 190 ºC was established in order to favor the paraffin wax decomposition. Subsequently, a second step at 450 ºC where HDPE degrades was proposed. The cycle took place under argon atmosphere to prevent the oxidation of metallic powder. However, the introduction of an air flux during the isothermal step of higher temperature promoted the complete elimination of decomposition products. The decomposition rates were experimentally determined taking into account the thickness of green bodies. As a result, this cycle lasted only 4 hours.

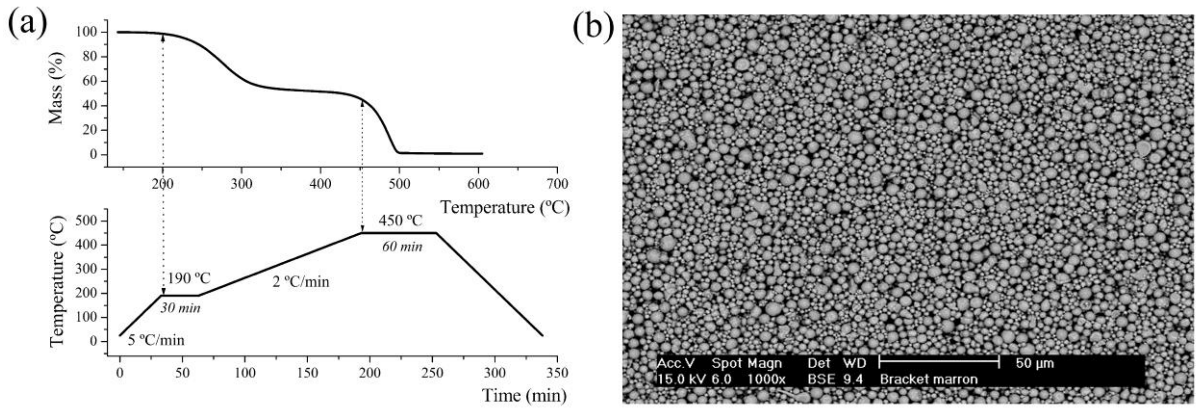

FIGURE 8. (A) TGA VS THERMAL DEBINDING CYCLE; (B) SCANNING ELECTRON MICROGRAPH OF BROWN PARTS.

Fig. 8(b) shows a scanning electron micrograph of a brown part where no remains of binder can be found. This homogeneous distribution of different sized metallic particles allowed a good sintering activity. After thermal debinding, defect-free parts were obtained and all of them preserved the shape of green bodies. The introduction of air during the second step of debinding cycle allowed to successfully eliminate the binder, avoiding an excess of carbon in the stainless steel powder.

3.4 Sintering

Brackets were sintered at 1250 ºC in low vacuum and pycnometer density reached near full density (98%). This densification degree showed that closed porosity in sintered parts is negligible. The microstructure of the duplex stainless steel brackets after sintering is presented in Fig. 9. The image was taken with BSE detector and three different contrasts can be distinguished. Black contrast corresponds to remaining pores, and bright and dark ones are assigned to ferrite and austenite phases characteristics of DSS. These phases were also confirmed by the different amount of nickel by EDS.

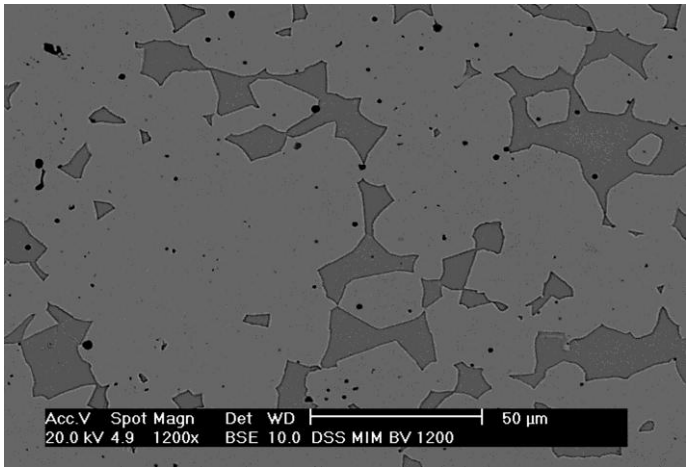

FIGURE 9. MICROSTRUCTURE OF INJECTION-MOULDED DUPLEX STAINLESS STEEL SINTERED AT 1250 ºC.

The linear shrinkage of brackets obtained in this work was around 10% and small differences in this value were found along the piece and were attributed not to the process but the geometry of the part. The linear shrinkage found in bending and tensile parts of 316L powder (d_{90} < 6 µm) of 1 mm in thickness obtained by µ-PIM was close to 13% [30]. The production of micro-rod arrays of 316L with a diameter of 100 µm employing a powder with an average particle size of 3 µm was consulted in literature [31], and in this case, the linear shrinkage was close to 15% and the relative density to 97%.

IV. CONCLUSIONS

Duplex stainless steel dental brackets were successfully produced by micro-powder injection moulding. This kind of steel is presented as an advantageous material for this application and µ-PIM is a profitable method to obtain micro-parts in order to avoid complicate machining steps. A developed thermoplastic binder constituted of high density polyethylene and paraffin wax was employed to obtain feedstocks with different powder loadings. According to oil absorption experimental method,

the CPVC for this system is 71 vol.%, and a similar result was found applying Reddy rheological model. All feedstock compositions presented pseudoplastic flow behaviour, with n ranges between 0.47 and 0.65, which are suitable for injection moulding. The most suitable feedstock to carry out the injection stage was selected according to torque and rheological measurements. The optimum powder loading of feedstock was 65 vol.% and its viscosity remained under 1000 Pa·s in the shear rate range between 100 and 1000 s^{-1}. The optimization of injection parameters allowed an accurately reproduction of the geometry of the mould. Green brackets were thermally debound employing a thermal cycle no longer than 4 hours. After sintering, brackets reached a 10% of linear shrinkage and relative density close to 98%. The employment of this technology to obtain duplex stainless steel brackets represents a fruitful contribution to orthodontics and materials fields.

ACKNOWLEDGEMENTS

Authors thank financial support received from MINECO (MAT2013-46452-C4-3-R project) and regional CAM government (MATERYENER P2013/MIT-2753 program). They also thank Centro Tecnológico Tekniker for its cooperation in the injection moulding stage.

REFERENCES

[1] F. Petzoldt, "Micro powder injection moulding – challenges and opportunities", Powder Injection Moulding International, vol. 2, no. 1, pp. 37-42, 2008.

[2] R. M. German, Powder Injection Moulding, MPIF, Princeton, NJ, 1990.

[3] R. K. Enneti, S. J. Park, A. Schenck, R. M. German, P. Thomas, B. Levenfeld, A. Varez, I. O. P. de Souza, J. P. de Souza, A. M. Fuentefria, V. P. Onbattuvelli and S. V. Atre, "Critical issues in manufacturing dental brackets by powder injection molding" Int. J. Powder Metall., vol.48, no. 2, pp. 23-29, 2012.

[4] P.Thomas, B. Levenfeld, A. Varez and A. Cervera, "Production of alumina microparts by powder injection moulding", Int. J. Appl. Ceram. Technol., vol. 8, no. 3, pp. 617-626, 2011.

[5] Lee. Y-K., "Translucency of dental ceramic, post and bracket", Materials, vol. 8, no. 11, pp. 7241-7249, 2015.

[6] K. T. Oh, S. U. Choo, K. M. Kim and K. N. Kim, "A stainless steel bracket for orthodontic application", Eur. J. Orthodont., vol. 27, pp. 237-244, 2005.

[7] K. T. Oh, Y. S. Kim, Y. S. Park and K. N. Kim, "Properties of super stainless steels for orthodontic applications", J. Biomed. Mater. Res. Part B, vol. 69B, pp. 183-194, 2004.

[8] A. Kocijan, D. K. Merl and M. Jenco, "The corrosion behaviour of austenitic and duplex stainless steels in artificial saliva with the addition of fluoride", Corrosion Science, vol. 53, no. 2, pp. 776-783, 2011.

[9] R. A. Lula, Stainless Steels, 5th ed., American Society for Metals, USA, 1993.

[10] P. Datta and G. S. Upadhyaya, "Sintered duplex stainless steels from premixes of 316L and 434L powders", Mater. Chem. Phys., vol. 67, pp. 234-242, 2001.

[11] T. Marcu Puscas, A. Molinari, J. Kazior, T. Pieczonka and M. Nykiel, "Sintering transformations in mixtures of austenitic and ferritic stainless steel powders", Powder Metall., vol. 44, no. 1, pp. 48-52, 2001.

[12] M. Campos, A. Bautista, D. Cáceres, J. Abenójar and J. M. Torralba, "Study of the interfaces between austenite and ferrite grains in P/M duplex stainless steels", J. Eur. Ceram. Soc., vol. 23, pp. 2813-2819, 2003.

[13] L. A. Dobrzański, Z. Brytan, M. A. Grande, M. Rosso and E. J. Pallavicini, "Properties of vacuum sintered duplex stainless steels", J. Mater. Process. Technol., vol. 162-163, pp. 286-292, 2005.

[14] C. J. Múñez, M. V. Utrilla and A. Ureña, "Effect of temperature on sintered austeno-ferritic stainless steel microstructure", J. Alloy. Compd., vol. 463, pp. 552-558, 2008.

[15] C. García, F. Martín, Y. Blanco, M. P. de Tiedra and M. L. Aparicio, "Influence of sintering under nitrogen atmosphere on microstructures of powder metallurgy duplex stainless steels", Metall. Mater. Trans. A-Phys. Metall. Mater. Sci., vol. 40A, pp. 292-301, 2009.

[16] R. Mariappan, S. Kumaran and T. Srinivasa Rao, "Effect of sintering atmosphere on structure and properties of austeno-ferritic stainless steels", Mater. Sci. Eng. A-Struct. Mater. Prop. Microstruct. Process, vol. 517, pp. 328-333, 2009.

[17] M. E. Sotomayor, B. Levenfeld and A. Várez, "Powder injection moulding of premixed ferritic and austenitic stainless steel powders", Mater. Sci. Eng. A-Struct. Mater. Prop. Microstruct. Process, vol. 528, pp. 3480-3488, 2011.

[18] N. Harradine, "The history and development of self-ligating brackets", Seminars in Orthodontics, vol. 14, no. 1, pp. 5-18, 2008.

[19] S. M. Lee and C. J. Hwang, "A comparative study of frictional force in self-ligating brackets according to the bracket-archwire angulation, bracket material, and wire type", Korean J. Orthod., vol. 45, no. 1, pp. 13-19, 2015.

[20] M. E. Sotomayor, A. Várez and B. Levenfeld, "Influence of powder particle size distribution on rheological properties of 316 L powder injection moulding feedstocks", Powder Technol., vol. 200, no. 1-2, pp. 30-36, 2010.

[21] G. Herranz, B. Levenfeld, A. Várez and J. M. Torralba, "Development of new feedstock formulation based on high density polyethylene for MIM of M2 high speed steels", Powder Metall., vol. 48, no. 2, pp. 134-138, 2005.

[22] L. Liu, N. H. Loh, B. Y. Tay, S. B. Tor, Y. Murakoshi and R. Maeda, "Mixing and characterisation of 316L stainless steel feedstock for micro powder injection molding", Mater. Charact., vol. 54, no. 3, pp. 230-238, 2005.

[23] G. P. Bierwagen, "CPVC Calculations. Journal of Paint Technology", vol. 44, no. 574, pp. 46-55, 1972.

[24] B. C. Mutsuddy and R. G. Ford, Ceramic Injection Molding, Chapman and Hall, London, UK, 1995.

[25] J. J. Reddy, N. Ravi and M. Vijayakumar, "A simple model for viscosity of powder injection moulding mixes with binder content above powder critical binder volume concentration", J. Eur. Ceram. Soc., vol. 20, no. 12, pp. 2183-2190, 2000.

[26] B. D. Coleman, H. Markovitz and W. Noll, Viscosimetric Flows of Non-newtonian Fluids, Springer-Verlag, New York, 1956.

[27] W. Ostwald, "Ueber die Geschwindigkeitsfunktion der Viscositatet disperser Systeme", Kolloid-Zeitschrift, vol. 36, pp. 99-128, 1925.

[28] A. De Waele, "Viscometry and plastometry", Journal of the Oil and Colour Chemists´ Association, vol. 6, pp. 33-69, 1923.

[29] B. C. Mutsuddy, "Injection Moulding Research Paves Way to Ceramic Engine Parts", Industrial Research and Development, vol. 25, pp. 76-80, 1983.

[30] C. Quinard, T. Barriere and J. C. Gelin, "Development and property identification of 316L stainless steel feedstock for PIM and µPIM", Powder Technol., vol. 190, no. 1-2, pp. 123-128, 2009.

[31] B. Y. Tay, L. Liu, N. H. Loh, S. B. Tor, Y. Murakoshi and R. Maeda, "Characterization of metallic micro rod arrays fabricated by µMIM", Mater. Charact., vol. 57, pp. 80-85, 2006.